



**HAL**  
open science

# The impact of common impurities present in gypsum deposits on in situ dissolution kinetics

Imen Zaier, Joel Billiotte, Laurent de Windt, Arnaud Charmoille

► **To cite this version:**

Imen Zaier, Joel Billiotte, Laurent de Windt, Arnaud Charmoille. The impact of common impurities present in gypsum deposits on in situ dissolution kinetics. *Environmental Earth Sciences*, 2023, 82 (1), pp.31. 10.1007/s12665-022-10710-4 . hal-03936681

**HAL Id: hal-03936681**

**<https://minesparis-psl.hal.science/hal-03936681>**

Submitted on 5 Dec 2023

**HAL** is a multi-disciplinary open access archive for the deposit and dissemination of scientific research documents, whether they are published or not. The documents may come from teaching and research institutions in France or abroad, or from public or private research centers.

L'archive ouverte pluridisciplinaire **HAL**, est destinée au dépôt et à la diffusion de documents scientifiques de niveau recherche, publiés ou non, émanant des établissements d'enseignement et de recherche français ou étrangers, des laboratoires publics ou privés.

# The impact of common impurities present in gypsum deposits on in situ dissolution kinetics

Imen Zaier<sup>1\*</sup>, Joël Billiotte<sup>2</sup>, Laurent De Windt<sup>2</sup>  
and Arnaud Charmoille<sup>1</sup>

<sup>1\*</sup>National Institute for Industrial Environment and Risks (Ineris), Rue Jacques Taffanel, Verneuil-en-Halatte, 60550, Hauts-de-France, France.

<sup>2</sup>Centre de Géoscience, MINES ParisTech, PSL University, 35 rue Saint-Honoré, Fontainebleau, 77300, Île-de-France, France.

\*Corresponding author. E-mail(s): [imen.zaier@ineris.fr](mailto:imen.zaier@ineris.fr);  
Contributing authors: [joel.billiotte@mines-paristech.fr](mailto:joel.billiotte@mines-paristech.fr);  
[laurent.dewindt@mines-paristech.fr](mailto:laurent.dewindt@mines-paristech.fr); [arnaud.charmoille@ineris.fr](mailto:arnaud.charmoille@ineris.fr);

## Abstract

This study aims to bring elements of understanding of water-gypsum interactions in situ to better assess the development of dissolution cavities in areas where gypsum is present at depth. Different types of natural gypsum facies are tested, impure alabaster, sacharoidal and clay/carbonate matrices gypsum. An experimental protocol is first developed to study the effect of erosion and particle transport on gypsum dissolution. An original leaching experiment under constant flow is first elaborated to study the effect of erosion and particle transport on the dissolution of gypsum. The flow of released particles is globally low and mostly composed of solid impurities (insolubles). The distribution of insolubles at the water-gypsum interface is found to have a significant impact on the dissolution. Geochemical models are then used to investigate the influence of the most common minerals present in natural gypsum on the dissolution process and the chemical composition of groundwater at their contact. These findings, applied to in situ conditions, allow us to evaluate the relevance of the common use of a simple criterion such as dissolved sulfate content or electrical conductivity to identify a system saturated in gypsum. Lastly, an effective

recession rate, derived from the dissolution rate and evaluated directly according to the groundwater saturation index of gypsum, is used to determine the intensity of natural gypsum dissolution in the study area.

**Keywords:** Dissolution mechanisms, Geochemical modeling, Particular transport, Recession rate, Underground cavities

## 1 Introduction

The development of natural dissolution processes of gypsum in the subsoil is still active in the Île-de-France region (France). This can have an impact on the population and infrastructures. Disturbances induced by construction activities, especially the underground ones, can accelerate dissolution and trigger disorders from disrupted or depressed areas generated by earlier dissolution events [1–3]. In this context, one of the iconic events is the discovery of a gypsum cavity in 1975 under Paris-Nord railway station, where the subsoil is rich with gypsum, that revealed a failure migrating up through the cover rocks [4]. It was induced by a continuous pumping of the aquifer of Eocene age for over a century. Another example can be found in urban areas around the northeast suburbs of Paris (Sevran and Villepinte) where recent and numerous collapses of the ground were caused by the development of underground cavities.

This study is part of a research and development project on gypsum dissolution mechanisms and associated ground movements in areas where gypsum is present at depth. We focus on the dissolution of natural gypsum located in the Eocene geological formation (56My - 34My) in the Seine-St-Denis department, about fifteen kilometers northeast of Paris. This area is characterized by a high population density, resulting in significant urbanization that generates an increase in traffic and therefore an increased demand on infrastructure. Therefore, our work should be used to predict and to prevent the gypsum dissolution, to quantify the key parameters of water-gypsum interactions and to manage underground construction projects accordingly in the concerned areas. One of the major projects in progress is the Grand Paris Express, the largest transport project in Europe designed to connect the suburbs of the Île-de-France region in France.

Generally, the natural dissolution of gypsum in the subsoil is a slow process but it is difficult to quantify its kinetics as a result of variable facies, accessory minerals, and hydro-geochemical conditions. Most of the knowledge on the dissolution kinetics of gypsum comes from laboratory studies performed at the mineral gypsum-solution interface such as rotating disk setups or flow cell devices, which quantify the dissociation rate of the gypsum mineral under well-controlled flow conditions [5–10]. More recent experiments employ atomic force measurements [11, 12] or holographic interferometry [13, 14] to characterize kinetic processes at a nanometric scale. These previous studies often use gypsum samples under ideal conditions (powder, polished or cleaved gypsum

crystals with a high purity criterion) and the solvent used is often pure water to have only the effect of the solubility of the mineral. Under such conditions, the dissolution rate is maximized and its application to the natural environment requires an upscaling scheme that includes the surface texture and conditions generated by the dissolution [15, 16].

Gypsum rocks in the natural environment are mainly composed of the mineral gypsum  $\text{CaSO}_4 \cdot 2\text{H}_2\text{O}$ , but they can be highly variable, as they can be mixed with other sedimentary minerals like carbonates, quartz, or clays [17] that we will refer to as solid impurities or insolubles. In case of active dissolution, this variability can lead to the modification of the rock surface geometry through the development of a roughness induced by the dissolution and governed by the underground water composition and its flow. This roughness induces a flow disturbance that changes the dissolution rate. Some progress has been made in a previous study [18], but it mainly consists of using a roughness factor that is not quantifiable from the considered gypsum properties.

In a previous publication, Zaier *et al.* (2021) [19] quantified the dissolution kinetics at the scale of gypsum samples with different porosities and contents of solid impurities. A rotating disk experiment was conducted under unconventional rigorous conditions to account for the effect of roughness developed during gypsum dissolution. The dissolution rate expression used is derived from non-linear mixed reaction-transport kinetic theory to consider the evolution of extensive fissures in karst aquifers under normal hydrogeological conditions. These determined rate laws could be used in numerical modelling approaches to study gypsum dissolution underground and the induced geomechanical consequences at the surface, such as depressions, subsidence, or sudden collapses [20–22].

The values of effective dissolution rates were found between 2 and 12  $\text{mg}/\text{m}^2/\text{s}$  [19] depending on the initial solution composition, the temperature as well as the texture, mineralogy, and even the crystalline properties, of the natural gypsum. These values are lower than the dissociation rate of the gypsum mineral found in the literature [23–26] due to coupled surface reaction and diffusion–controlled kinetics. However, these rates were found to be in the same order of magnitude when compared to the data obtained under the same hydrodynamic conditions of [27]. The effect of porosity on the dissolution rate was found to be insignificant in the presence of solid impurities [28]. The results of those unconventional rotating disk experiments mainly included the effect of roughness and insolubles and provided for a global quantification of dissolution rates under natural undisturbed hydrogeological conditions. The determined dissolution rates were different compared to the values provided by a dissolution kinetic model based on an ideal flat water-rock interface [29, 30]. These low values of experimental or simulated dissolution rates led to question the assumption that the natural dissolution was the only process responsible for the formation of dissolution cavities.

This paper investigates whether particle detachment during dissolution can enhance the progressive evolution of the underground void and contribute to

the destabilization of a dissolution cavity. First, a novel lab protocol is designed to better determine the contribution of the particles released in the quantification of the dissolution time evolution (recession rate) by integrating the porosity and the insolubles fraction of several natural gypsum samples. The results of the laboratory experiments are then extended to the in situ conditions by geochemical modeling of water-rock interactions in the range of groundwater flow velocities. The effects of the most common minerals present in gypsum deposits and the groundwater chemistry are assessed. These modeling results will be an important element for a thorough analysis of the water saturation state of a gypsum aquifer in the concerned area. A range of recession rate values "in situ" is defined as function of the gypsum facies on the one hand, and the groundwater saturation index determined from groundwater chemical analysis on the other hand.

## 2 Materials and Methods

### 2.1 Materials

The Société du Grand Paris (SGP), in charge of piloting the Grand Paris Express project, provided the drilling campaign data considered in this study, in particular the data from the section of the future subway line between the communes of Sevran and Livry-Gargan in the Seine-Saint-Denis department where gypsum is present at depth.

Field cores were taken during the exploration campaign and stored in the core shack of the Société du Grand Paris. These cores showed a broad petrographic diversity of natural gypsum rocks in terms of crystalline forms and grain sizes. We focus on gypsum deposits mainly concentrated in two Eocene formations [31]: (a) the "gypsum masses and interstratified marls" of Ludian (Priabonian) age (37 My-34 My) where gypsum forms , (b) the "marls and loose stones" of Lutetian age (46 My-40 My). Four main homogeneous facies were identified [19]:

- sacharoidal gypsum with a crystallized sugar appearance, located in the 1<sup>st</sup> and 2<sup>nd</sup> masses of the Ludian (Priabonian) formation.
- matrix gypsum with a carbonate-clay texture, located in the 3<sup>rd</sup> and 4<sup>th</sup> gypsum masses of the Ludian (Priabonian) formation,
- alabaster gypsum with a compact milky-white appearance, extracted from the Lutetian formation,
- impure alabaster gypsum with greyish appearance, extracted from the Lutetian formation.

For each of these facies, samples were taken with visually different contents of insolubles, but they all present homogeneous appearance at the decimetric scale which potentially ensures the absence of centimeter-scale heterogeneities of the samples used in the laboratory.

The petrographic and petrophysical properties of those facies are summarized in Table 1. Porosity was measured by triple-weight method and

mercury porosimetry. Grain size was determined by scanning electron microscope (SEM) observations of thin sections and by Dino-Lite high-resolution digital microscope observations of the sample surface (Figure 1). Insolubles fraction was determined by weighting the residues left after dissolving a sample of crushed gypsum rock. These insolubles were present in significant quantities ( $> 10\%$ ) for impure alabaster gypsum and matrix gypsum. Their mineralogy was determined by X-ray diffraction (XRD). The insolubles within the samples were composed of quartz, calcite, magnesian calcite and ferro-dolomite. Sacharoidal gypsum contained traces of ankerite ( $\text{Ca}(\text{Fe},\text{Mg},\text{Mn})(\text{CO}_3)_2$ ), matrix textured gypsum traces of anhydrite, and alabaster and sacharoidal gypsum traces of clays.

**Table 1** Mineralogical and petrophysical properties of the studied gypsum samples.

Facies	porosity $\phi$ (%)	grain size ( $\mu\text{m}$ )	insolubles fraction $F_i$ (%)	insolubles composition
Sacharoidal gypsum	8 - 12	120 - 510	5 - 11	quartz, calcite, Mg-calcite, Fe-dolomite, ankerite, clays
Matrix-textured gypsum	17 - 25	140 - 1000	14 - 19	quartz, calcite, Mg-calcite, Fe-dolomite, anhydrite
Alabaster gypsum	$< 1$	210 - 2000	2.6	quartz, calcite, Mg-calcite, Fe-dolomite, clays
Impure alabaster gypsum	1 - 3	100 - 250	15	quartz, calcite, Mg-calcite, Fe-dolomite



**Fig. 1** Facies of the studied gypsum sampled observed with the Dino-Lite digital microscope.

In a previous publication, Zaier *et al.* (2021) [19] studied the effect of the different petrophysical parameters on the dissolution rate for each gypsum facies. The texture of the facies and the spatial distribution of insolubles have an important effect on the dissolution kinetics, whereas porosity has only significant effect for gypsum with low insoluble particles.

The dissolution process can lead to a detachment of gypsum grains or insoluble materials by a deconstruction and/or erosion mechanism depending on the rock texture. The transport of these solid particles by the fluid in contact can contribute to the growth of a dissolution cavity [32]. Estimating the resistance to erosion for each gypsum facies requires a reliable experimental set-up to collect the grains released by gypsum dissolution, to quantify the mass and nature of the grains, and to characterize the particulate flow.

## 2.2 Methods

### 2.2.1 Experimental Protocol

The evaluation of erosion and particle transport related to gypsum dissolution was carried out by performing leaching tests to determine the mass and nature of the released grains. The experiment consisted in entirely immersing a block of gypsum in a horizontal canal with a low water flow velocity (0.05 cm/s and 5 cm/s) to promote a vertical fall of the grains released by dissolution instead of their dragging.

The flow canal (Figure 2a) was subjected to a number of test runs to establish the proper configuration for uniform flow conditions and optimal collection of the released particles. This canal has a form of a gutter with a width of 7.8 cm and a depth of 4 cm, i.e. a section of 31.2 cm<sup>2</sup> and a length of 51 cm. A pipe connected to the running water ensured a constant flow through a throttling valve and a distribution grid located at 4 cm from the upstream limit of the canal. A transparent window located in the central part allowed to observe the lateral side of the gypsum block subjected to dissolution. A spillway (preceded by a distribution grid located 4 cm upstream) kept a constant water level at the downstream end of the canal.

The gypsum sample was shaped like a parallelepiped with a length of 6 cm, a width of about 2 cm and a height of about 3 cm, to ensure a uniform flow at the surfaces subjected to dissolution. The width was reduced to 1 cm over a height of 5 mm in its lower part. A coating with epoxy resin delimited the surfaces exposed to dissolution leading to a lateral strip with a height of 2 cm (Figure 2b). The resin overlay covered the top surface, as well as the surfaces defining the foot and the back side. The front face was not covered to maximize the flow on the exposed sides. This surface was affected by dissolution, but less intensively than the side surfaces due to the ending of the streamlines on its surface. The particle flow produced by this face could make a partial contribution to the two lateral ones.

A system was placed under the submerged block in the canal to capture the sediments released vertically. However, the finest particles were difficult to be trapped. In the early experiments, the collection system attached to the base of the channel under the block took the form of a cylindrical container with an inlet diameter of 5.5 cm and a height of 5.5 cm (Figure 2a). Its axis was located 27 cm from the upstream side of the canal. The block was placed asymmetrically, +1 cm towards the front and +0.5 cm towards the back to

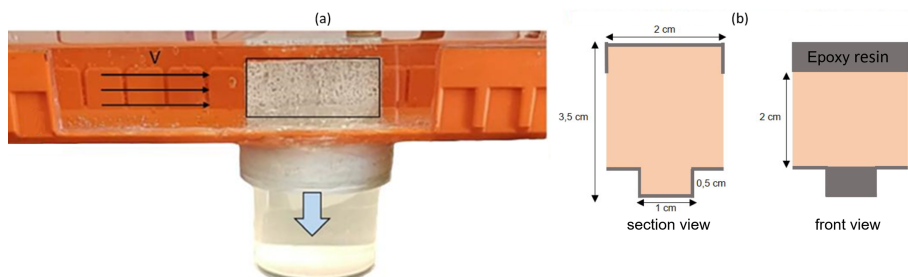


**Fig. 2** (a) Fully flooded gypsum block subjected to water flow velocity of 0.1 to 1 cm/s inside a canal with particle collector; (b) cross section and front view of the gypsum block.

avoid collecting the particles released from the front side or from areas near the back side where dissolution can be disturbed by the resin coating. Consequently, the collected particle masses had to be multiplied by a correction factor to normalize them to the total lateral area. An optical tracking of the collected grains during each leaching experiment was performed by taking a photograph of the bottom of the collection container every 12 hours.

The collection container was filled with a fluid that prevented the dissolution of the released gypsum grains. A solution saturated with gypsum was preferred to organochlorine solvent. The latter was not efficient because of the interfacial tension and the wettability of the particles that stopped their circulation through the water-solvent interface. Furthermore, a gypsum-saturated solution did not present any environmental and safety constraints unlike solvents. However, its saturation capability decreased during the experiment by diffusive or even convective exchange with the flow in the canal. To limit such a saturation decreased at the collected particles level, the height of the trap was adjusted so that the variation in the degree of saturation by simple diffusion is less than 5% during a 10-day period. This led to a tripling of the height of the container compared to the view presented in Figure 2a, i.e., 16.5 cm. Eventually, a fine pipette of the saturated solution was added each 3 days to restore gypsum saturation for long experiments.

The grains present into the collector were recovered by filtration using a cellulose nitrate membrane filter of  $0.2 \mu\text{m}$  at the end of the dissolution experiment. The particles were dried, weighted, and then observed with a microscope (up to  $32\times$ ) and/or with a Dino-Lite digital microscope (up to  $250\times$ ) to determine their granulometry. Their mineralogy was determined by XRD, but the very low masses recovered resulted in a rather high uncertainty.

These tests were carried out with the gypsum facies mentioned in subsection 2.1. Pure alabaster gypsum did not release any particles. The used flow velocities were 0.1 and 1 cm/s to avoid excessive drag of the finest grains. The leaching time for the sacharoidal and impure alabaster gypsum blocks was set to 7 days. However, this duration was increased to 21 days for the matrix textured gypsum block due to the clear reduction of the dissolution kinetics by coating effect. Complementary experiments carried out at higher flow velocities (beyond 1 cm/s) could not be finalized because of the difficulty to trap

the grains released by dissolution and to maintain a saturation state in the collector.

## 2.3 Geochemical modeling

The evaluation of the effect of the mineralogy of insolubles on gypsum dissolution at the laboratory scale is then extended to the in-situ conditions by geochemical modeling of water-rock interactions. The geochemical model used is CHESS of the reactive transport code HYTEC [33], designed to simulate the equilibrium state of complex aquatic systems, including minerals and gases. The database used is WATEQF [34] based on truncated Davies model for activity correction. The truncated Davies is a variant of the Debye-Hückel equation that is accurate to ionic strengths up to 0.3 - 0.5 M and is commonly applied in the geochemical modeling of natural water [35].

The saturation index (SI) of the solution with respect to a given mineral was calculated as:

$$SI = \log\left(\frac{Q}{K_s}\right) \quad (1)$$

where  $Q$  is the ion activity product and  $K_s$  is the solubility constant. A SI of 0 means that the mineral is in thermodynamic equilibrium with the aqueous solution. A negative SI means that the mineral (if present) can dissolve, whereas a positive SI means that the mineral can be formed (precipitate) from the aqueous solution.

The dissolution/precipitation kinetics of a mineral  $M$  was modeled according to the following law:

$$\frac{d[M]}{dt} = kS_v\left(\frac{Q}{K_s} - 1\right)^n \quad (2)$$

where  $[M]$  is the mineral concentration (e.g. mg/L),  $k$  is the intrinsic kinetic rate constant (e.g. mg/m<sup>2</sup>/s),  $S_v$  is the reactive surface area of the mineral (e.g. m<sup>2</sup>/L), and  $n$  is an empirical exponent. The term  $\left(\frac{Q}{K_s} - 1\right)$ , or equivalently  $(10^{SI} - 1)$ , expresses the effect of the saturation state on the kinetics (if  $Q < K_s$ : dissolution, if  $Q > K_s$ : precipitation).

The dissolution rate constants of gypsum were experimentally determined in a previous study by the unconventional rotating disc technique at a temperature of 15°C [19]. The initial solution used is the tap water of the distribution system of Fontainebleau. This water has a chemical composition close to that of natural waters of aquifers surrounding common gypsum facies found in Ile-de-France and its main components are linked to calcite equilibrium ( $[\text{HCO}_3^-] = 310 \text{ mg/L}$ ;  $[\text{Ca}^{2+}] = 115,3 \text{ mg/L}$ ;  $[\text{SO}_4^{2-}] = 34,5 \text{ mg/L}$ ). The dissolution rate constants found in the previous study [19] are the following:

$$k = 8.7 \text{ mg/m}^2/\text{s} ; \quad n = 1.13 \quad \text{for sacharoidal gypsum} \quad (3a)$$

$$k = 3.6 \text{ mg/m}^2/\text{s} ; \quad n = 1.21 \quad \text{for matrix textured gypsum} \quad (3b)$$

$$k = 5.1 \text{ mg/m}^2/\text{s} ; n = 1.10 \quad \text{for alabaster gypsum} \quad (3c)$$

$$k = 8.9 \text{ mg/m}^2/\text{s} ; n = 1.14 \quad \text{for impure alabaster gypsum} \quad (3d)$$

To simplify the geochemical modeling, the mineral phases of insolubles had the same specific surface area as gypsum ( $4.31 \times 10^{-5} \text{ m}^2/\text{g}$ ) and were composed of calcite  $\text{CaCO}_3$  and the disordered dolomite  $\text{CaMg}(\text{CO}_3)_2$ . The latter stood for a proxy of the magnesian calcite ( $\text{Ca}_{1-x}\text{Mg}_{1+x}(\text{CO}_3)_2$ ) that was present in all the studied gypsum facies. The solubility of these insolubles enriched the solution in magnesium but also in calcium which is a common ion with gypsum. Therefore, calcium input by the insolubles disturbed gypsum solubility.

## 3 Results and discussion

### 3.1 Influence of erosion and particle transport

The pictures taken from the collection container during each leaching experiment were difficult to manage due to the low production of particles, their dispersion at the bottom of the container and the perturbations of their distribution by the added gypsum-saturated solution. However, two phases of grain release could be identified. The first phase was characterized by no, or very low, release of insolubles. This first period of dissolution was related to initially flat surfaces exposed to the flow and presenting a recession sufficient to highlight insoluble particles until particle detachment. In a second phase, grains detached from the rock in packets and fell into the container bottom, after one day for the sacharoidal and impure alabaster gypsum, and two days for the matrix textured gypsum. Pure alabaster gypsum was not included in the analyses because it does not produce particles.

For the considered gypsum blocks, the mass of the collected particles turned out to be low to very low compared to the total mass loss. This corresponded to very low values of particulate flows, relatively to the immersion time in the flow canal, even while considering that the release of particles was only effective after a necessary period to allow release by erosion or deconstruction. The amount of gypsum grains in the collected masses was not very important, i.e., from 0 to 20% for sacharoidal and impure alabaster, respectively. These quantities remained marginal compared to the amount of dissolved gypsum. A proportion close to 30% was measured for the matrix textured gypsum, but it corresponded to a very low particle production due to the retention of the matrix even after the dissolution of main gypsum grains. The observed gypsum particles seemed to be released from small gypsum grains embedded in the matrix (Figure 3).

For sacharoidal gypsum, there was no evidence of gypsum grains being released by dissolution at the grain boundaries. The dissolution induced a continuous recession of the surface exposed to the flowing water with a small relief of insolubles in the form of yellowish flakes that could be more important if present in continuous form or in localized coherent masses (Figure 4a

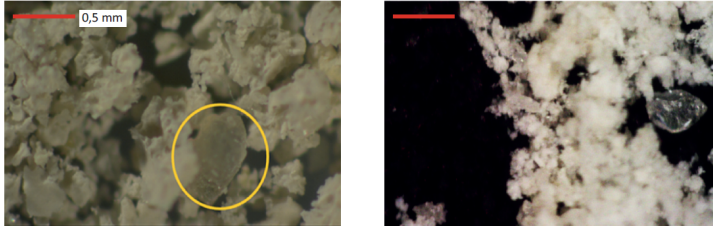


**Fig. 3** Binocular observations of trapped grains from matrix textured gypsum blocks.

and 4b). Under these conditions, insoluble particles disturbed the flow and locally amplified the dissolution without increasing the release of grains. However, this effect was not important compared to the simple consideration of the flow related to gypsum solubilization, because of the low initial content of insolubles (<10%). For the impure alabaster gypsum with a higher insolubles fraction (15%), insolubles created macroscopic reliefs during the dissolution that also resisted against the erosion induced by the flow velocities. They presented a relatively small thickness. Gaps corresponding to portions of released insoluble were also observed. Only the marks of the solid impurities were left in small reliefs on the face of the dissolving gypsum surface (Figure 4c).

Only the matrix-textured gypsum, which had a higher initial content in insolubles, produced a significant proportion of gypsum in the order of 20 to 30%. This gypsum was associated to a release of small grains embedded in the matrix due to the matrix dissolution. However, this matrix strongly slowed down the dissolution by coating effect and the depth of the dissolution front remained small. Destructuration by dissolution or erosion of this matrix was not observed, except for the clay (Figure 4d).

In the matrix dominated by carbonate, a sudden mechanical destructuration of a large volume (where only the matrix remained) could be conceived. Such a scenario could not be quantified by a continuous particle flow additional to dissolution. This residual matrix with a highly aerated texture might exhibit a mechanical instability, due to the significant loss of solid mass by dissolution in the order of 70%. The collapse of the residual matrix could lead to the instant creation of a clear void. Table 2 summarizes the surface observations of the different gypsum facies, the particle flow and the ratio of the global mass of the collected grains to that of the global mass loss after dissolution.

Despite the numerous experimental tests, the results did not show clear evidence of an entrainment or a release of gypsum grains either by erosion or by destructuration of the material capable of enhancing the dissolution processes, especially for sacharoidal gypsum. The values of the dissolution rates and the particle flow varied with the flow velocity for each gypsum facies. The values of the dissolution coefficient ( $\text{mg}/\text{m}^2/\text{s}$ ) determined for a 1 cm/s velocity are consisted with those determined by the unconventional rotating disc technique at zero velocity [19] with a difference ranging from 5 to 50%. These deviations are much smaller compared to those determined for the 0.1 cm/s velocity due to the high erosion caused the rotational speeds used (50 to 200 rpm).

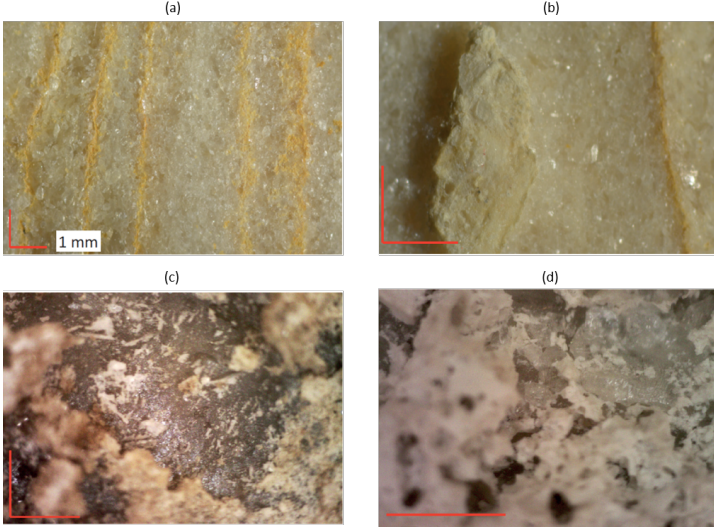


**Fig. 4** Binocular observations of the dissolved surface of natural gypsums: (a) yellow streak marks (sacharoidal facies), (b) small mass of insolubles not affected by dissolution (sacharoidal facies), (c) small relief due to the attachment of insolubles on the face of the dissolving gypsum surface, (d) gypsum grains covered by a layer of insolubles and highlighted by a recession of the clay matrix during dissolution.

**Table 2** Surface observations of gypsum facies, particle flow and the mass ratio after dissolution.

gypsum facies	particular flow	surface observations	mass ratio (%)
sacharoidal	+	regressive dissolution	-
	++	streak marks ①      insoluble mass ②      regressive dissolution ③	4-6
impure alabaster	+++	insoluble matrix ①      regressive dissolution ②      ①	12
carbonate matrix	+	dissolution of gypsum grains at the surface ①      erosion of the matrix ②	4
clay-carbonate matrix	+++	dissolution of gypsum grains at the surface ①	6

The dissolution process can be characterized by a dissolution rate that quantifies the time evolution of dissolution. This rate is commonly called the recession rate and it depends on the porosity  $\phi$  and the density  $\rho$  of the gypsum facies as follows:

$$\tau_{r0} = \frac{k}{\rho(1 - \phi/100)} \quad (4)$$

The contribution of particles released by dissolution can be incorporated in the recession rate by introducing the insolubles fraction  $F_i$  in addition to the porosity. This allows to better evaluate a recession rate that represents a proper in situ value considering the long-term sensitivity of insolubles to erosion and, hence, the mineralogical and hydrogeological context in the natural

environment. The new recession rate equation then becomes:

$$\tau_r = \frac{\tau_{r_0}}{(1 - F_i/100)} \quad (5)$$

For alabaster gypsum of low insolubles fraction ( $F_i \approx 3\%$ ), the recession created by dissolution did not lead to a release or entrainment of insoluble particles. Therefore, the value of the recession rate in situ should not account for insoluble particles ( $\tau_{r_0}$ ). For sacharoidal gypsum of few insoluble particles ( $F_i \leq 10\%$ ), particles are released and carried away continuously by the flow. The recession rate in situ is, therefore, more representative when weighted by the insoluble particles ( $\tau_r$ ). For gypsum facies with high insoluble particles ( $F_i > 10\%$ ) that are more or less sensitive to erosion, the limited duration of the experiments did not allow a complete release of the insolubles. The use of the value of the recession rate weighted by the insoluble particles may be representative of a long-term evolution with a significant development of the total dissolved volume. It does not take into account the influence of their resistance to erosion. It is then proposed to use as in situ value the average between the weighted and unweighted recession rates by insoluble particles. ( $(\tau_r + \tau_{r_0})/2$ ). The gypsum with carbonate matrix texture was not sensitive to erosion and no evidence of a continuous solid dissolution flow was detected. However, the mobility of the insoluble matrix can occur in a delayed and instantaneous manner in the form of mechanical instability. It is then not possible to define a constant dissolution flow of the solid phase related to the production of particles without characterizing the properties of the residual matrix. The knowledge of these parameters would make it possible to estimate a critical volume and thus an approximate duration of the particle release process and the creation of the void. Without these properties, the proposed recession rate does not consider the insoluble particles ( $\tau_{r_0}$ ).

The values of the in situ recession rates range from 1 to 6 nm/s which maximizes the natural in situ dissolution rate of zones where flow velocities are lower the water flow velocity of 1 cm/s in the experiments. That only excludes the close vicinity of an anthropic hydrological disturbance with high water velocities. The few available values of water flow velocities in gypsum aquifers result from tracing experiments carried out in gypsum karst in mountainous areas: about 0.03 to 0.3 cm/s in the French Alps [36], 0.4 to 12 cm/s in the Ukrainian Carpathians [37, 38], up to about 14 cm/s in the Italian Alps [39]. High velocities related either to karst-type circulation or to the proximate field of an anthropogenic disturbance induce larger shear forces that would increase the influence of erosion. The use of the defined values would then have to be evaluated according to the sensitivity of the facies present to erosion.

### 3.2 Influence of solid impurities present in gypsum deposits

Based on the experimental results, the influence of the minerals potentially present in the gypsum (calcite, dolomite) on its dissolution and on the composition of the groundwater in contact with it is determined by geochemical modelling. The consideration of the kinetic laws of the different mineral species in the simulations allows to estimate the evolution of the dissolution process at long times, more representative of the real conditions in situ.

The solubility of calcite is low, about 0.06 g/L in a system open to the atmosphere (i.e. a partial pressure in carbon dioxide,  $p\text{CO}_2$ , of 0.0004 atm), compared to that of gypsum ( $\approx 2500$  mg/L) and therefore, it does not play a significant role on gypsum dissolution whether it is present as insolubles or in an under-saturated condition in the solution. At thermodynamic equilibrium, the effect of gypsum on the dissolution/precipitation of calcite in pure water is determined by increasing the saturation index of gypsum by equimolar dissolution of  $\text{CaSO}_4 \cdot 2\text{H}_2\text{O}$ . Figure 5 shows that the dissociation of gypsum by dissolution increases the concentration of calcium ion in the solution, leading to the precipitation of calcite by approximately 60% of the initial amount dissolved. This precipitation is, therefore, limited by the quantities of bicarbonates present in the solution, and it only modifies the mass of dissolved gypsum very marginally.

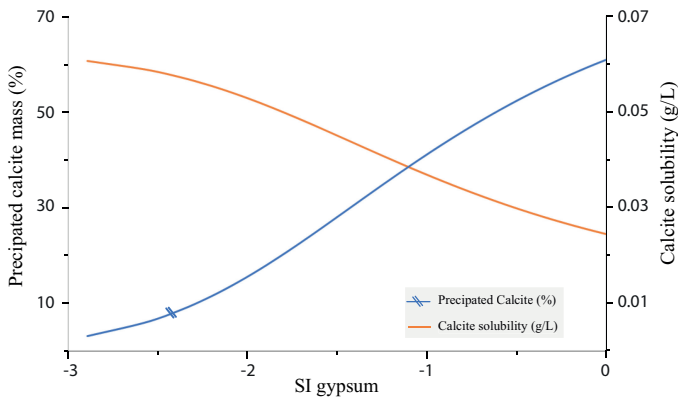


**Fig. 5** Effect of gypsum on the dissolution/precipitation of calcite.

On the other hand, the presence of dolomite increases the solubility of gypsum to about 3300 mg/L as shown in Figure 6. The stoichiometry of the dissolved dolomite (one atom of calcium for one of magnesium) results in an increase of magnesium concentrations in the solution and an excessive amount of calcium. This leads to a precipitation of calcite, limited however by the quantity of bicarbonates resulting from dolomite. Figure 6 illustrates the mass loss of dolomite and the mass increase of calcite relative to the initial mass in the solution as the gypsum saturation index increases. With a form of

dolomite more stable, this mechanism of dolomite-calcite transformation would be identical but slower and limited in fact by magnesium concentration.

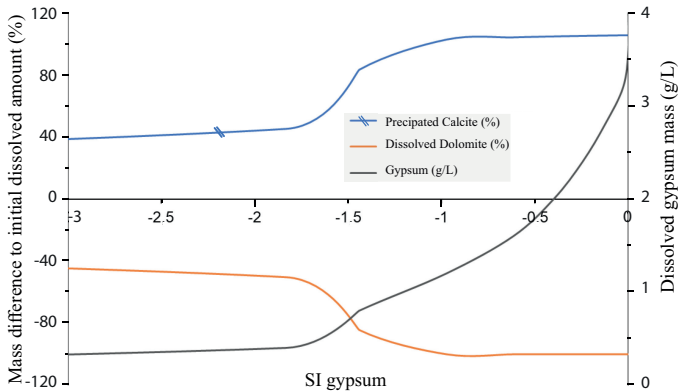


**Fig. 6** Effect of dolomite on the solution composition and gypsum dissolution.

In the study area, we identified areas that seemed to be oversaturated with gypsum due to very high sulfate concentrations ( $> 1600$  mg/L), well above the reference value usually taken as a criterion to identify a gypsum saturated system (1400 - 1450 mg/L). Geochemical modelling has been carried out at long times (100 years) and in a system closed to the atmosphere, i.e., corresponding to natural conditions ( $PCO_2=0.01$  atm), to study if the presence of high amounts of sulfate is related to the interaction of magnesian calcite with gypsum. The consideration of gypsum kinetics in addition to those of dolomite and calcite in the simulations shows a dolomite-calcite transformation which continues even after reaching equilibrium with gypsum, because of the slow kinetics of dolomite compared to that of gypsum. This leads to an excess of magnesium due to the dissolution of dolomite, and a calcium deficit due to the precipitation of calcite, which is compensated by an increase in sulfate concentrations to maintain the equilibrium with gypsum. Calcite precipitation occurs more rapidly than dolomite dissolution, mainly due to the presence of calcium ions from gypsum dissolution. Geochemical simulations in a closed system show an asymmetric evolution of calcite and dolomite content during the first 20 years in contact with water (Figure 7).

The dissolution of the dolomite continues, and it induces an increase in calcium concentration that is compensated by a simultaneous precipitation of calcite and a high concentration of sulfate and magnesium as illustrated in Figure 7. The concentrations of sulfate become higher than 1600 mg/L and can even reach 1900 mg/L in 100 years and the  $Ca^{2+}/SO_4^{2-}$  molar ratio becomes different from 1. This compensation results in a symmetrical evolution of the masses of calcite and dolomite, and a precipitation of magnesite  $MgCO_3$ . For geological timescales, the extrapolation of this symmetrical behavior would lead to a total transformation of the initially present dolomite. The influence

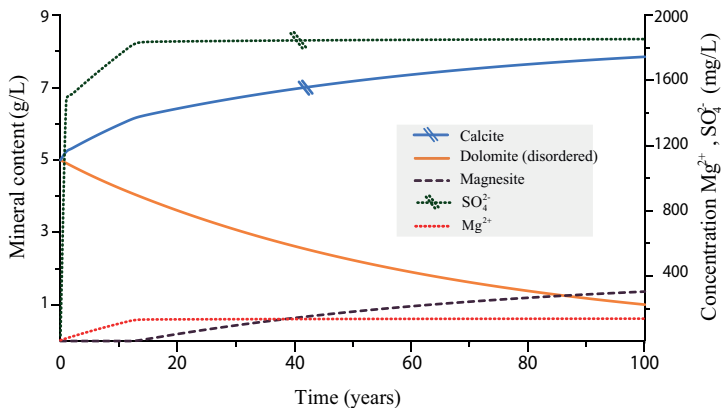


**Fig. 7** Dolomite-calcite transformation in a closed system over 100 years.

of magnesite is not considered because of its rare presence in the studied area and its chemical composition with no common ions with gypsum.

### 3.3 Influence of groundwater composition and saturation status

The dissolution process into gypsum deposits is commonly linked to chemical composition of water intakes from aquifers without gypsum or natural rainoff infiltration. Aquifers of the study area are mainly carbonated. So incoming waters are mineralized and could present a significant amount of calcium ions.

In a mineralized water, the initial quantity of calcium in the solution induces a decrease of the final quantity of dissolved gypsum at equilibrium compared to the one expected in pure water by common ion effect with gypsum. This leads to a modification of the quantity of sulfate at equilibrium. Consequently, the knowledge of the initial quantity of calcium in the solution reduces the uncertainty on the final quantity of sulfate at equilibrium.

The influence of the initial presence of calcium in the solution on gypsum dissolution could be quantified by parametric simulations with calcium–bicarbonate waters of synthetic composition. These waters are composed of various amounts of calcium and bicarbonates ranging from 10 to 300 mg/L (Table 3). For each of these pairs of values, the equilibrium concentrations of calcium and bicarbonates are determined for a temperature of 13°C and a partial pressure of CO<sub>2</sub> equal to 0.01 atm, close to the average in situ values of the studied area. This first equilibrium is often associated with a precipitation of calcite, which modifies the pH and the concentrations of calcium and bicarbonates. The values of these three quantities define the calcium–bicarbonate water in contact with the gypsum. The results presented in Table 3 show that by adding gypsum, the reaction induces a significant increase in the amount of calcium and, therefore, a decrease in the sulfate concentrations at

equilibrium down to 1200 mg/L, which is lower than the reference value generally used as a criterion to define a system saturated in gypsum (1400 - 1450 mg/L).

**Table 3** Effect of calcium-bicarbonate water on the quantity of calcium and sulfate ions at equilibrium with gypsum ( $\text{PCO}_2=0.01 \text{ atm}$ ).

initial cond.		initial solution				final solution			
$\text{Ca}^{2+}$ (mg/L)	$\text{HCO}_3^-$ (mg/L)	pH	$\text{Ca}^{2+}$ (mg/L)	$\text{SO}_4^{2-}$ (mg/L)	$\text{HCO}_3^-$ (mg/L)	pH	$\text{Ca}^{2+}$ (mg/L)	$\text{SO}_4^{2-}$ (mg/L)	$\text{HCO}_3^-$ (mg/L)
10	10	5.97	0	0	38	6.5	620	1486.6	65
100	100	6.93	100	0	127	6.96	679	1387	155
200	100	6.91	200	0	127	6.96	734	1294	155
300	100	6.90	300	0	127	6.96	808	1217	154
100	200	7.23	100	0	227	7.01	655	1436	169
200	200	7.14	188	0	197	6.99	720	1324	162
300	200	7.07	270	0	174	6.96	777	1250	160
100	300	7.31	80	0	265	7.02	646	1454	170
200	300	7.17	166	0	204	6.99	705	1346	163
300	300	7.09	252	0	180	6.97	764	1257	158

Thus, the amount of calcium initially present a calcium-bicarbonate water decreases gypsum solubility to maintain the thermodynamic equilibrium and increases the molar imbalance of calcium and sulfate (Figure 8). At gypsum equilibrium, the molar ratio  $\text{Ca}^{2+}/\text{SO}_4^{2-}$  is found to be significantly higher than 1 and can reach 1.6. The excessive amount of calcium in the solution implies a partial substitution of the dissolved gypsum mass by the precipitation of calcite crystals.

An indicator of gypsum-calcite substitution was found during a previous investigation conducted by Cerema on the composition of gypsum facies in the study area [40]. This work identified the presence of calcite in a crystallized form, usually mistaken for sacharoidal gypsum, but likely results from of the dissolution of gypsum and the precipitation of calcite in calcareous water with an initial high calcium concentration.

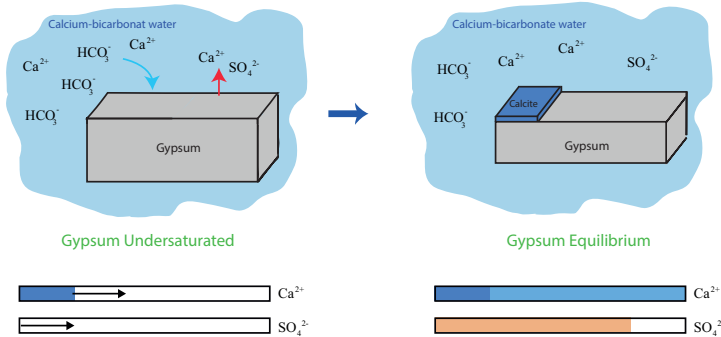


**Fig. 8** Schematic representation of gypsum dissolution mechanism in calcium-bicarbonate water.

### 3.4 Quantification of in situ recession rates

The presence of dolomitic insolubles and the initial presence of significant amounts of calcium in the solution on gypsum dissolution lead respectively to an increase or a decrease in sulfate concentration at equilibrium. Therefore, the common using of sulfate concentration to evaluate the saturation index of groundwater with respect to gypsum could be erroneous. A more reliable evaluation must take into account these two biases by including at least  $Mg^{2+}$ ,  $Ca^{2+}$  and bicarbonate concentrations.

For each gypsum facies, the experimental measurements allowed to obtain the exponent of the kinetic law and to suggest values of the recession rate as a function of porosity,  $\phi$ , and insolubles fraction,  $F_i$ . It is then possible to define a range of recession rate values in situ as a function of the facies and the saturation index SI corresponding to the water composition. It is important to keep in mind that the calculation of this parameter involves several assumptions and associated uncertainties and that we are more interested in its variation than its absolute value, though the comparison of absolute values at a single site makes it possible to compare the intensities of dissolution processes between different sites.

Considering groundwater with gypsum saturation indices between -1.5 and 0, the results presented in Figure 9 mostly indicate a quasi-linear evolution of the "in situ" recession rate values, at least while SI is higher than 0.75. This apparent linearity is related to the value of the exponent  $n$  close to unity. For a given SI gypsum, the set of points varies according to the porosity and insolubles range. The upper limit indicates the rate for maximum porosity and insolubles range and the lower limit indicates the rate for minimum porosity and insolubles range.

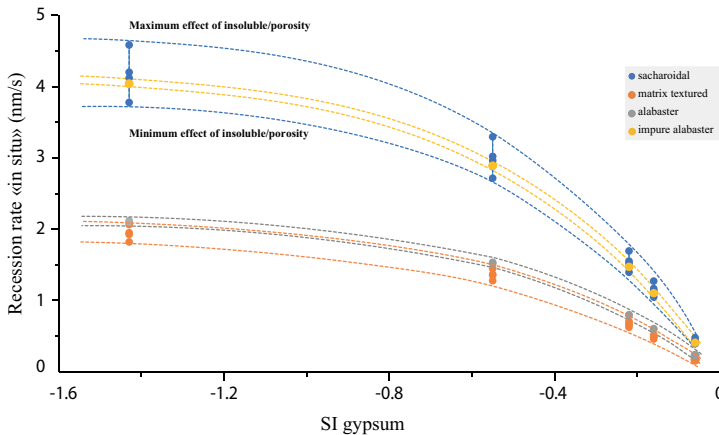


**Fig. 9** Recession rate evolution as a function of the saturation index (SI) for each gypsum facies of the studied area.

In an under-saturated system with water flow lower than 1cm/s, the values of the recession rate for the different gypsum facies vary between 1.8 and 4.6 nm/s, i.e., between 5.7 and 14.5 cm/y. These variations decrease when the saturation state of the system with respect to dissolved gypsum increases. Impure alabaster gypsum could exhibit recession rates that are twice as great as those of pure non-porous alabaster gypsum depending on the distribution of insolubles on the surface exposed to dissolution (relief effect). As for matrix textured gypsum, it presents a rate about twice lower than that of sacharoidal gypsum because of the covering effect by the clay-carbonate matrix which limits the dissolution kinetics. However, this effect is underestimated for high flow velocities because the protective carbonate-clay matrix might not resist and its instantaneous detachment would uncover the gypsum grains, increase the depth of penetration, and modify the recession velocity.

To conclude, the analysis tool generally used to identify an active dissolution area which is based on the use of a simple criterion, such as sulfate concentration or electrical conductivity, is not sufficient. This is because it does not allow to establish neither the water saturation state of a gypsum aquifer, nor the quantity of dissolved gypsum to quantify the dissolution rate. It is then necessary to conduct a chemical analysis of the water and define a gypsum SI to be associated with the facies to determine a recession rate according to the texture of the gypsum rock present in the concerned area. This value needs to be determined from a complete chemical analysis and not only from the sulfate concentration because of the interactions between gypsum dissolution, bicarbonates and calcium content and the potential presence of magnesian calcite.

## 4 Conclusion

The impact of erosion and particle transport related to gypsum dissolution was determined by controlled leaching tests with a constant low flow velocity (0.1 and 1 cm/s) involving a collection of the released grains. For each gypsum facies tested, the particulate flow was found low to very low compared to dissolved mass flow. It is composed mostly of insolubles with only rare small gypsum gains. The distribution of insolubles at the interface was found to have a large influence on the dissolution. Despite numerous experimental tests, the results did not show a role of entrainment or release of gypsum grains by erosion that could be added to the dissolution process as a result of the destructureation of the material and increase the cavity creation kinetics. This is the case in particular for the sacharoidal gypsum, which is the most common in the Paris region. For gypsum with highly porous matrix, the progression of dissolution within the pores remained shallow, even with increasing the leaching time, and this is due to the deceleration of dissolution by coating effect. The flow velocities used did not lead to sudden matrix destructureation, as might occur in situ with a dissolution affecting a large volume. We did observe erosion of the matrix when it is mainly composed of clays.

For each studied gypsum facies, the experiments allowed an evaluation of the recession rate that considered the release of particles present in the sample by dissolution. This rate can be used for the simulation of natural dissolution in the range of in situ velocities and outside the field of immediate disturbances related to underground structures.

To extend the experimental results to in situ conditions, the influence of the mineralogy of the insoluble particles and the groundwater composition and saturation status on the dissolution process was studied by geochemical modeling. This work revealed the limitations of using a simple criterion to characterize the water saturation state in a gypsum aquifer, such as sulfate concentration (1400 - 1450 mg/L) or electrical conductivity (2.2 mS/cm). Additional variables such as calcium/sulfate mole ratio and/or magnesium concentration should be considered. These variables allow to evaluate the effect of the initial presence of significant amounts of calcium and bicarbonates related to the partial pressure in carbon dioxide  $\text{PCO}_2$  as well as the influence of dolomitic insolubles. Both effects have been studied by modeling and lead to a reduction or an increase of the gypsum solubility, respectively:

- Dissolution of gypsum in calcium bicarbonate water induces a decrease in gypsum solubility. The sulfate concentrations can reach 1200 mg/L to respect the mass action law of gypsum at equilibrium. The solutions corresponding to these conditions are characterized by a  $\text{Ca}^{2+}/\text{SO}_4^{2-}$  mole ratio significantly higher than 1, i.e., reaching 1.6.
- The dissolution of natural gypsum containing dolomitic insolubles reveals on an in situ scale a dolomite-calcite transformation that keeps on going slowly, even if the thermodynamic equilibrium with gypsum is reached. This leads to an excess of magnesium (100 - 150 mg/L) supplied by the dissolution of dolomite, and a deficit of calcium because of calcite precipitation, which is balanced by an increase in sulfate concentrations, above 1600 mg/L and up to 1900 mg/L. The gypsum solubility will, therefore, increase under these conditions.

In-situ measurements, laboratory experiments and modeling work have led to a better understanding of the intensity of natural gypsum dissolution phenomena and the potential factors leading to its further development. A method was developed to propose orders of magnitude of in situ recession rates as a function of the groundwater saturation level with respect to gypsum and the petrophysical characteristics of the gypsum facies: porosity and solid impurities. In the studied context, the natural dissolution processes remain relatively "slow", and the recession rates were found between 0 and 4.6 nm/s in the laboratory, i.e., between 0 and 14.5 cm/y, for SI gypsum between 0 and -1.5. These results can be used to simulate the development of underground voids by dissolution, based on a model combining geochemical reactions, flow and transport.

## Acknowledgements

This research work was supported by Ineris in the framework of a partnership with the Société du Grand Paris which financially supported a part of this study and facilitated access to data and core samples collected during the geological and hydrogeological characterization of the future Grand Paris Express subway line.

## References

- [1] Chardon, M., Nicod, J.: Gypsum Karst of France. *International Journal of Speleology* **25**(3-4), 203–208 (1996). <https://doi.org/10.5038/1827-806X.25.3.15>
- [2] Klimchouk, A., Andrejchuk, V.: Environmental problems in gypsum karst terrains. *International Journal of Speleology* **25**(3-4) (1996). <https://doi.org/10.5038/1827-806X.25.3.11>
- [3] Thierry, P., Prunier-Leparmentier, A.-M., Lembezat, c., Vanoudheusden, E., Vernoux, J.-F.: 3d geological modelling at urban scale and mapping of ground movement susceptibility from gypsum dissolution: The Paris example (France). *Engineering Geology* **105**, 51–64 (2009)
- [4] Toulemont, M.: Les Gypses Lutétiens du Bassin de Paris Sédimentation, Karstification et Conséquences Géotechniques, Géotechnique-mécanique des sols-sciences de la terre GT-24 edn. Rapports des laboratoires. LCPC, France (1987)
- [5] Barton, A.F.M., Wilde, N.M.: Dissolution rates of polycrystalline samples of gypsum and orthorhombic forms of calcium sulphate by a rotating disc method. *Transactions of the faraday society* **67**, 3590–3597 (1971). <https://doi.org/10.1039/TF9716703590>
- [6] Lebedev, A.L., Lekhov, A.: Dissolution kinetics of natural-gypsum in water at 5–25°C. *Lomonosov Moscow State University* **27**, 85–94 (1990)
- [7] Klimchouk, A.: Dissolution and conversions of gypsum and anhydrite **25**(3), 21–36 (1996). <https://doi.org/10.5038/1827-806X.25.3.2>
- [8] Wang, F., Davis, T.E., Tarabara, V.V.: Crystallization of Calcium Sulfate Dihydrate in the Presence of Colloidal Silica. *Industrial & Engineering Chemistry Research* **49**(22), 11344–11350 (2010). <https://doi.org/10.1021/ie100309b>
- [9] Lebedev, A.L.: Kinetics of gypsum dissolution in water. *Geochemistry International* **53**(9), 811–824 (2015). <https://doi.org/10.1134/S0016702915070058>

- [10] Dai, Z., Kan, A.T., Shi, W., Zhang, N., Zhang, F., Yan, F., Bhandari, N., Zhang, Z., Liu, Y., Ruan, G., Tomson, M.B.: Solubility measurements and predictions of gypsum, anhydrite, and calcite over wide ranges of temperature, pressure, and ionic strength with mixed electrolytes. *Rock Mech Rock Eng* **50**, 327–339 (2016). <https://doi.org/10.1007/s00603-016-1123-9>
- [11] Burgos-Cara, A., Putnis, C.V., Rodriguez-Navarro, C., Ruiz-Agudo, E.: Hydration effects on gypsum dissolution revealed by in situ nanoscale atomic force microscopy observations. *Geochimica et Cosmochimica Acta* **179**, 110–122 (2016). <https://doi.org/10.1016/j.gca.2016.02.008>
- [12] Zareepolgardan, B., Piednoir, A., Colombani, J.: Gypsum Dissolution Rate from Atomic Step Kinetics. *Journal of Physical Chemistry C, American Chemical Society* **17**(121), 9325 (2017). <https://doi.org/10.1021/acs.jpcc.7b00612>
- [13] Colombani, J., Bert, J.: Holographic interferometry study of the dissolution and diffusion of gypsum in water. *Geochimica et Cosmochimica Acta* **71**(8), 1913–1920 (2007). <https://doi.org/10.1016/j.gca.2007.01.012>
- [14] Feng, P., Brand, A.S., Chen, L., Bullard, J.W.: In situ nanoscale observations of gypsum dissolution by digital holographic microscopy. *Chemical Geology* **460**, 25–36 (2017). <https://doi.org/10.1016/j.chemgeo.2017.04.008>
- [15] Sadeghiamirshahidi, M., Vitton, S.J.: Analysis of drying and saturating natural gypsum samples for mechanical testing. *Journal of Rock Mechanics and Geotechnical Engineering* (2018). <https://doi.org/10.1016/j.jrmge.2018.08.007>
- [16] Fattah, M., Habeeb, I., Omran, H.: A study on leaching of collapsible gypseous soils. *International Journal of Geotechnical Engineering*, 1–11 (2019). <https://doi.org/10.1080/19386362.2019.1647664>
- [17] Marteau, P.: *Mémento roches et minéraux industriels Gypse et anhydrite*. Technical report, BRGM, Orleans, France (1993)
- [18] Colombani, J.: Dissolution measurement free from mass transport. *Pure and Applied Chemistry* **85**(1), 61–70 (2012). <https://doi.org/10.1351/PAC-CON-12-03-07>
- [19] Zaier, I., Billiotte, J., Charmoille, A., Laouafa, F.: The dissolution kinetics of natural gypsum : a case study of Paris Eocene facies in the north-eastern suburbs of Paris. *Environmental Earth Sciences* **80**(8) (2021). <https://doi.org/10.1007/s12665-020-09275-x>

- [20] Laouafa, F., Guo, J., Quintard, M.: Modeling of salt and gypsum dissolution: applications, evaluation of geomechanical hazards. *European Journal of Environmental and Civil Engineering* **25**, 1405–1426 (2018). <https://doi.org/10.1080/19648189.2019.1579758>
- [21] Moore, K., Holländer, H., Basri, M., Roemer, M.: Application of geochemical and groundwater data to predict sinkhole formation in a gypsum formation in manitoba, canada. *Environmental Earth Sciences* **78** (2019). <https://doi.org/10.1007/s12665-019-8188-1>
- [22] Laouafa, F., Guo, J., Quintard, M.: Underground rock dissolution and geomechanical issues. *Rock Mechanics and Rock Engineering* **54**, 1–23 (2021). <https://doi.org/10.1007/s00603-020-02320-y>
- [23] Liu, S.-T., Nancollas, G.H.: The kinetics of dissolution of calcium sulfate dihydrate. *Journal of Inorganic and Nuclear Chemistry* **33**(8), 2311–2316 (1971). [https://doi.org/10.1016/0022-0248\(76\)90247-5](https://doi.org/10.1016/0022-0248(76)90247-5)
- [24] Bolan, N.S., Syers, J.K., Sumner, M.E.: Dissolution of various sources of gypsum in aqueous solutions and in soil. *Journal of the Science of Food and Agriculture* **57**(4), 527–541 (1991). <https://doi.org/10.1002/jfsa.2740570406>
- [25] Raines, M.A., Dewers, T.A.: Mixed transport reaction control of gypsum dissolution kinetics in aqueous solutions and initiation of gypsum karst. *Chemical Geology* **140**(1–2), 29–48 (1997). [https://doi.org/10.1016/S0009-2541\(97\)00018-1](https://doi.org/10.1016/S0009-2541(97)00018-1)
- [26] Jeschke, A.A., Vosbeck, K., Dreybrodt, W.: Surface controlled dissolution rates of gypsum in aqueous solutions exhibit nonlinear dissolution kinetics. *Geochimica et Cosmochimica Acta* **65**(1), 27–34 (2001). [https://doi.org/10.1016/S0016-7037\(00\)00510-X](https://doi.org/10.1016/S0016-7037(00)00510-X)
- [27] Colombani, J.: Measurement of the pure dissolution rate constant of a mineral in water. *Geochimica et Cosmochimica Acta* **72**(23), 5634–5640 (2008). <https://doi.org/10.1016/j.gca.2008.09.007>
- [28] Zaier, I.: Rôle du transport particulaire lié à la déstructuration de gypses poreux dans le développement de cavités de dissolution. PhD thesis, Université PSL, MINES ParisTech (Feb. 2021). p.207
- [29] Vieillefon, J.: Contribution of the improvement of the analysis of gypsiferous soils. *Materials Sciences* **17**(3), 195–223 (1979)
- [30] Jeschke, A.A., Dreybrodt, W.: Dissolution rates of minerals and their relation to surface morphology. *Geochimica et Cosmochimica Acta* **66**(17), 3055–3062 (2002). [https://doi.org/10.1016/S0016-7037\(02\)00893-1](https://doi.org/10.1016/S0016-7037(02)00893-1)

- [31] Egal, E., Kreziak, c., Saitta, A., Marlinge, J., Priol, G.: Methodology for the detection of unstructured zones and cavities in parisian gypsum underground along the line 16 of the grand paris express (france). AFTES International Congress (2017)
- [32] Charmoille, A., Lecomte, A., Kreziak, C.: Gypsum Natural Dissolution processes-Assessment and Management of Subsidence and Collapse Hazards, p. 34. Ineris & Cerema, Île-de-France, France (2018)
- [33] Van der Lee, J., De Windt, L., Lagneau, L., Goblet, P.: Module-oriented modeling of reactive transport with HYTEC. *Computers & Geosciences* **29**, 265–275 (2003). [https://doi.org/10.1016/S0098-3004\(03\)00004-9](https://doi.org/10.1016/S0098-3004(03)00004-9)
- [34] Plummer, L.M., Jones, B.F., Truesdell, A.H.: Wateqf-a computer program for calculating chemical equilibrium of natural waters. Technical report, U.S. Geological Survey, Washington DC, USA (1976). <https://doi.org/10.3133/wri7613>
- [35] Bethke, C.M.: *Geochemical and Biogeochemical Reaction Modeling: Second Edition*, p. 546. Cambridge University Press, University of Illinois Urbana-Champaign (2008)
- [36] Couturier, B., Fourneaux, J.-C., Sommeria, L.: Conditions of underground water circulation in the gypsum karsts of the french inner Alps. *Karstologia* **33**, 51–58 (1999)
- [37] Klimchouk, A.: Hydrogeology of gypsum formations. *International Journal of Speleology* **25**(3-4), 83–89 (1996). <https://doi.org/10.5038/1827-806X.25.3.6>
- [38] Klimchouk, A., Aksem, S.: Hydrochemistry and solution rates in gypsum karst: Case study from the western ukraine. *Environmental Earth Sciences* **48**(3), 307–319 (2005). <https://doi.org/10.1007/s00254-005-1277-3>
- [39] Vigna, B., D’Angeli, I., Fiorucci, A., De Waele, J.: Hydrogeological flow in gypsum karst areas: Some examples from northern Italy and main circulation models. *International Journal of Speleology* **46**, 205–217 (2017). <https://doi.org/10.5038/1827-806X.46.2.2095>
- [40] Charmoille, A., Kreziak, C.: Caractérisation du système de dissolution du gypse Lutétien à Sevrans - Premiers résultats, p. 23. Ineris & Cerema, CFGI-CFMR, Île-de-France, France. [http://www.cfgi-geologie.fr/wp-content/uploads/2019/04/2019-02-07\\_6-CFGI-CFMR\\_Gypse-Sevrans\\_07-02-19-Def.pdf](http://www.cfgi-geologie.fr/wp-content/uploads/2019/04/2019-02-07_6-CFGI-CFMR_Gypse-Sevrans_07-02-19-Def.pdf)